COBEM 87 — IX Congresso Brasileiro de Engenharia Mecânica, Florianópolis, SC (Dezembro, 1987)
9th Brazilian Congress of Mechanical Engineering

Laminar Flow Through a Smooth Expansion: Comparison With a Bench-Mark Solution

C.R. MALISKA* e A.F.C. SILVA*

Depto. Engenharia Mecânica — UFSC
Cx. Postal 476 - 88049 - Florianópolis - SC

J.A.O. PEREZ*

Depto. Ingenieria Mecánica
Universidad de Magalhanes, Punta Arenas - Chile

ABSTRACT

A finite volume method written for general curvilinear coordinate systems is used to solve a test problem proposed by the Working Group on Refined Modelling of Flows, of the I.A.H.R., with the aim of testing the ability of the existing methods in dealing with fluid flow problems defined in arbitrary geometries. The results obtained compare very well with those of a bench-mark solution, listing the method described here among the best ones analysed by the Working Group.

INTRODUCTION

The procedure for obtaining the numerical counterpart of a partial differential equation involves several approximating steps. These steps, when well designed, leads to numerical techniques that produce exact solutions when the grid spacing tends to zero. Therefore, the numerical methods emerge as a fast and sophisticated tool for the solution of complex engineering problems. For the assesment and comparison of many different existing methods, and for checking purposes during the design phase of a numerical model, it is necessary to have high precision tabulated results, known as bench-mark solutions. A bench-mark solution of the two-dimensional natural convection problem in a square cavity has been reported in |1|. Since this geometry can be discretized using the Cartesian coordinate system, this bench-mark solution does not serve as a test problem for those methods which are designed to deal with arbitrary geometries.

To fulfill this requirement the Working Group on Refined Modelling of Flows of the International Association for Hydraulic Research, called for solutions of the two-dimensional laminar flow in a smooth expansion, proposed by Roache |2|, as shown in Fig. 1. As can be seen, the boundary of the domain does not fit to any conventional coordinate system, posing diffilcuties for the numerical methods written for fixed coordinate systems.

Two methodologies are widely employed for solving fluid flow problems; finite differences and finite elements. The following excerpt, from |3|, pictures the situation: "With regard to the specific task of computing flows in complex geometries, the finite element method appears as the most natural tool, owing to its intrinsic geometric flexibility. However, the finite difference method takes more and more advantage of co-ordinate transformations and grid generation techniques to exploit its superior simplicity and efficiency".

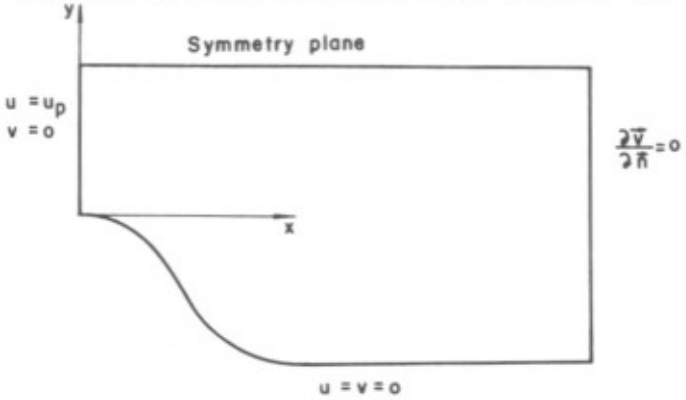

Fig. 1 Problem geometry - Re = 10.

As a result of the "call for solutions", eighteen solutions were received by the Working Group. They were analyzed, compared with a bench-march solution obtained by Cliffe et al |4| and reported with the details of each numerical model employed by Napolitano and Orlandi |3|.

In the present work the same test problem is solved using a boundary-fitted nonorthogonal model and the results compared with the bench-mark solution reported in |3|. This test offers a unique opportunity of comparing the perfomance of the model described in this work with several others developed around the world.

TEST PROBLEM

The plane channel flow proposed by Roache |2| and depicted in Fig.1, changes its geometry according to the value of the Reynolds number. For large Re number the channel becomes straighter and longer, as can be seen in Fig. 2. The south boundary (solid wall) of the channel is given by the following expression in the x-y coordinate system,

$$y_s(x) = [\tanh(2 - 30x/Re) - \tanh(2)]/2 \qquad (1)$$

where the x coordinate ranges from 0 to Re/3. The flow is laminar and incompressible with the boundary conditions shown in Fig. 1.

The mandatory cases selected for running were for Re=10 and Re=100. For Re=10 the channel results well distorted turning out to be a good test of the ability of the methods in capturing the recirculation region for this case. The Re=100 case serves for assessing the convergence rate of the models with increasing Re.

A 21 x 21 grid points finite difference mesh, or an equivalent finite element discretization, was required to be used in order to have all solutions on same basis.

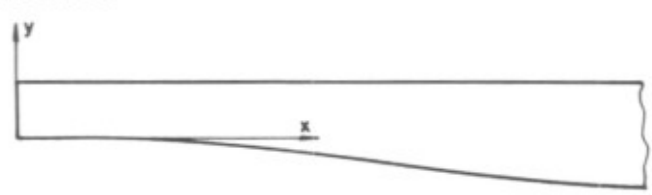

Fig. 2 Channel geometry - Re = 100.

*Member of ABCM

The governing equations for the problem, written in the Cartesian coordinate system are

$$\frac{\partial}{\partial x}(\rho u) + \frac{\partial}{\partial y}(\rho v) = 0 \tag{2}$$

$$\frac{\partial}{\partial x}(\rho uu) + \frac{\partial}{\partial y}(\rho vu) = -\frac{\partial P}{\partial x} + \frac{\partial}{\partial x}(\mu\frac{\partial u}{\partial x}) + \frac{\partial}{\partial y}(\mu\frac{\partial u}{\partial y}) \tag{3}$$

$$\frac{\partial}{\partial x}(\rho uv) + \frac{\partial}{\partial y}(\rho vv) = -\frac{\partial P}{\partial y} + \frac{\partial}{\partial x}(\mu\frac{\partial v}{\partial x}) + \frac{\partial}{\partial y}(\mu\frac{\partial v}{\partial y}) \tag{4}$$

The numerical method used in this work to solve the above system of equations is now addressed.

NUMERICAL METHOD

Since the main goal of this paper is to asses the numerical model employed here, it is important to give some of its details |5| |6|. The method is written for general curvilinear coordinates, where the boundary-fitted discretization can be either orthogonal or nonorthogonal being generated algebraically or through differential methods |7|.

To solve the problem in the new coordinate system the conservation equations, Eqs (2)-(4), are transformed to this system keeping its divergence form. The approximated algebraic equations are obtained by integration of the transformed equations for all elemental control volumes. Since the equations are in a conservative form this is equivalent of performing mass and momentum balances for the elemental control volumes, ending up in a finite volume methodology fully conservative. The volumes are now square elements with sides $\Delta\xi=\Delta\eta=1$.

The dependent variables in the Cartesian coordinate system, u, v, and P, are kept as dependent variables in the $(\xi-\eta)$ coordinate system. As discussed in details in |6|, to keep the Cartesian components of the velocity vector as dependent variables, forces the u and v velocity components to be calculated at all interfaces of a pressure control volume, as shown in Fig. 3, in order to perform the mass flow calculation through the boundaries of the control volume. The advantage in doing this is the simplicity of the resulting transformed equations. The transformed equations are

$$\frac{\partial U}{\partial \xi} + \frac{\partial V}{\partial \eta} = 0 \tag{5}$$

$$\frac{\partial}{\partial \xi}(\rho Uu) + \frac{\partial}{\partial \eta}(\rho Vu) = -\frac{\partial P}{\partial \xi} y_\eta + \frac{\partial P}{\partial \eta} y_\xi + \frac{\partial}{\partial \xi}(C_1\frac{\partial u}{\partial \xi} + C_2\frac{\partial u}{\partial \eta}) + \frac{\partial}{\partial \eta}(C_4\frac{\partial u}{\partial \eta} + C_5\frac{\partial u}{\partial \xi}) \tag{6}$$

$$\frac{\partial}{\partial \xi}(\rho Uv) + \frac{\partial}{\partial \eta}(\rho Vv) = -\frac{\partial P}{\partial \eta} x_\xi + \frac{\partial P}{\partial \xi} x_\eta + \frac{\partial}{\partial \xi}(C_1\frac{\partial v}{\partial \xi} + C_2\frac{\partial v}{\partial \eta}) + \frac{\partial}{\partial \eta}(C_4\frac{\partial v}{\partial \eta} + C_5\frac{\partial v}{\partial \xi}) \tag{7}$$

where U and V are the contravariant velocity components written without metric normalization, given by

$$U = y_\eta u - x_\eta v \qquad V = x_\xi v - y_\xi u \tag{8}$$

The next step to obtain the system of algebraic equations is to integrate Eqs. (5) - (7) over the respective elemental control volumes. Writing the aproximate equation for a general scalar ϕ one gets an equation of the form

$$A_P\phi_P^{n+1} = A_e\phi_E^{n+1} + A_w\phi_W^{n+1} + A_n\phi_N^{n+1} + A_s\phi_S^{n+1} + A_P\phi_P^n/(1+E) - L[\hat{P}^\phi]\Delta V + L[\hat{ST}^\phi]\Delta V \tag{9}$$

where ϕ stands for u and v and L [ ] represents the numerical approximation of the quantity inside the brackets. The mass conservation equation written for the elemental control volume shown in Fig. 3 is

$$(\rho U)_e - (\rho U)_w + (\rho V)_n - (\rho V)_s = 0 \tag{10}$$

Putting ϕ equal to u and v in Eq.(9) and using Eq. (8) one obtains the following approximated equations in terms of the contravariant velocities

$$U_P = \hat{U}_P - F_1(\Delta P) \qquad V_P = \hat{V}_P - F_2(\Delta P) \tag{11}$$

where the functions F_1 and F_2 involve the pressure gradients in the ξ and η directions. Details and expressions for the coefficients can be found in |5| and |6|.

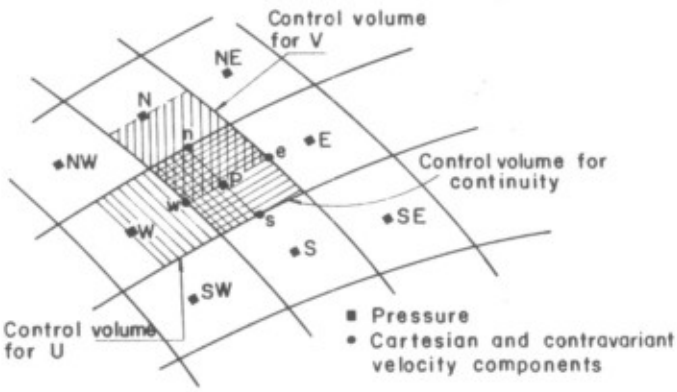

Fig. 3 Elemental control volume.

Since one is dealing with incompressible flows it is necessary to close the system of equations deriving an extra equation for pressure. The method employed to handle the pressure-velocity coupling problem ammounts in introducing Eq.(11) into Eq.(10), obtaining an equation for pressure of the form

$$A_PP_P = A_eP_E + A_nP_N + A_sP_S + A_wP_W + A_{ne}P_{NE} + A_{se}P_{SE} + A_{nw}P_{NW} + A_{sw}P_{SW} + B \tag{12}$$

The system of equations given by Eqs.(11) and (12) is solved in a segregated manner. Eq.(11) is solved in a point iteration fashion through the calculation of U and V using the best estimates of the u and v components, while Eq. (12) is solved using the S.O.R technique with over-relaxation. The convergence rate of the method is similar to that of methods designed for fixed coordinate systems |5| |6|.

In the next section the results obtained with this methodology are reported and compared with the bench-mark solution reported in |3|.

NUMERICAL RESULTS

For the Re=10 case two types of discretization were used, as shown in Figs. 4 and 5. The former one was obtained algebraically, while the later one was constructed using the method described in |7|, with

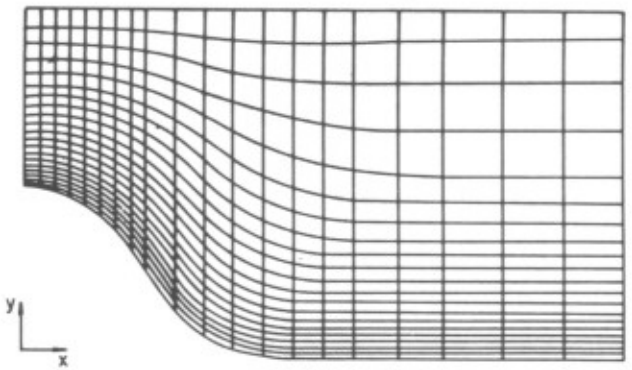

Fig. 4 Boundary-fitted discretization - Grid 1

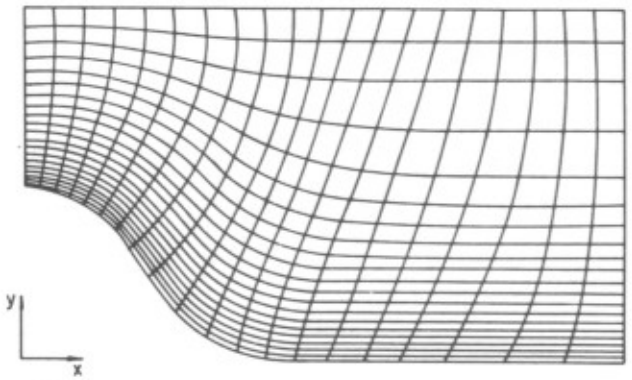

Fig. 5 Boundary-fitted discretization - Grid 2

the aim of making the grid quasi-orthogonal at the lower boundary.

The results reported in |3| are in terms of the vorticity and pressure at the solid wall. To calculated these variables at the wall second order profiles are constructed using the available internal points. The expression for the vorticity at the wall in the $\xi-\eta$ plane is given by

$$\omega = -J\left(\frac{\partial v}{\partial \eta} y_\xi + \frac{\partial u}{\partial \eta} x_\xi\right) \qquad (13)$$

where the values of the derivative of u and v are given by

$$\left.\frac{\partial u}{\partial \eta}\right|_f = 3u_3 - u_2/3 \qquad \left.\frac{\partial v}{\partial \eta}\right|_f = 3v_3 - v_2/3 \qquad (14)$$

where the velocity components involved in the above equations are depicted in Fig. 6.

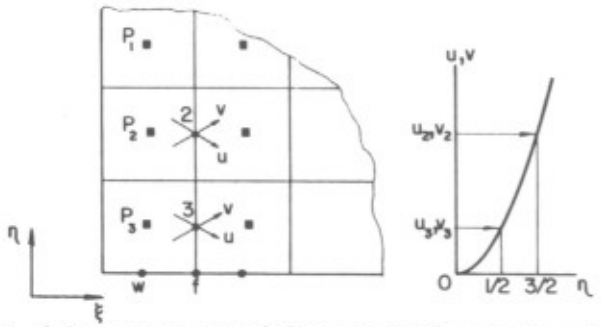

Fig. 6 Pressure and voticity calculation at the wall.

The pressure at the wall is calculated using the pressure points P_1 , P_2 and P_3 shown in Fig. 6.

Since the pressure level is immaterial in this problem the pressure was set to zero at X/X_{out} = 0.5, as established when the problem was proposed.

The way employed in |3| to measure the performance of the methods is given by the following expressions

$$\varepsilon_\omega = \frac{100}{19}\sum_{i=2}^{20}\left|\frac{\omega_i-\omega_i^*}{\omega_i^*}\right| \qquad \varepsilon_p = \frac{100}{18}\sum_{i=2}^{20}\left|\frac{P_i-P_i^*}{P_i^*}\right| \qquad (15)$$

where ε_ω and ε_p are the average errors in the vorticity and pressure calculations, ω_i and P_i are the vorticity and pressure values along the wall and the symbol (*) means the bench-mark solution of |4|. The vorticity and pressure at the inlet and outlet are not included in the error computation |3| since the boundary condition at the outlet was left to the choice of the participants, and the type of boundary condition used may influence the average significantly. At the inlet the vorticity is known and the pressure will depend on the boundary condition used for this variable. Since different methodologies were used to solve the problem the organizers felt that not including these points it would not penalize any participant.

The authors of this work feel that the use of Eq. (15) is not the proper way to measure the performance of the methods. The existence of a recirculation region brings the vorticity close to zero, and very small error in this region, wich have no significance in the overall solution, may result in a ε_ω value not representing the real performance. For this reason the results are plotted such that the overall behaviour can be compared with the bench-mark solution. Due to space restrictions the tabulated results are shown only for the vorticity for the Re=10 case, in Table I. The tables for the remainder cases can be found in |8|. The complete results including those of the bench-mark solution and those obtained by Hutton are shown in Figs. 7, 8, 9 and 10. It is important to point out that the results of Hutton are the best ones presented in the comparative work of |3|.

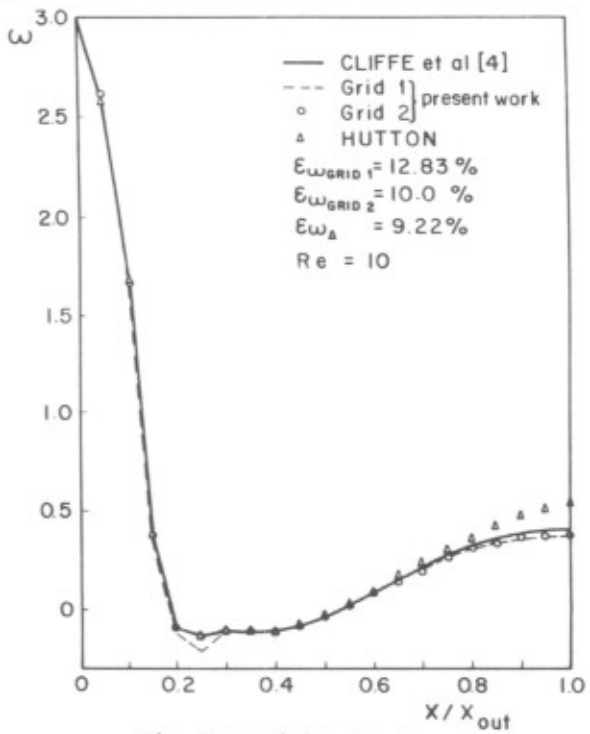

Fig. 7 Vorticity for Re = 10.

Inspecting Figs. 7 to 10, one sees that the results follow closely the bench-mark solution and the results of Hutton for both cases and for the whole range of the variable X . In fact, in Fig. 7 and 8 the results obtained with the Grid 2, are in better agreement with the bench-mark solution than the results of Hutton in the region close to the channel

exit. Another interesting finding can be appreciated in Fig. 8. In this plot, close to the channel

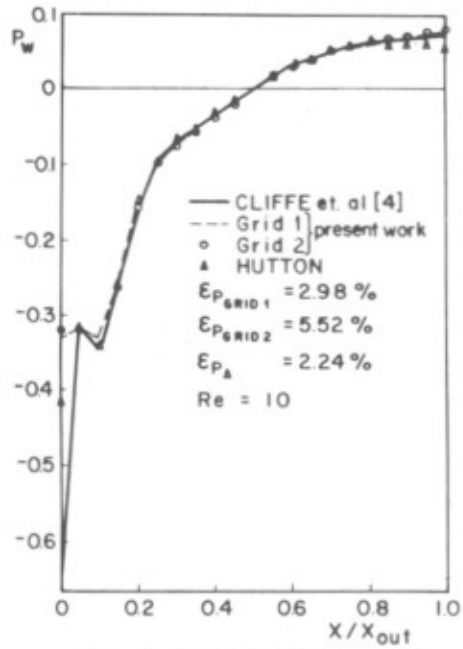

Fig. 8 Pressure for Re = 10.

entrance, the pressure obtained in this work, with both grids, are in good agreement with Hutton's results but not with that of the bench-mark solution.

Table I - Vorticity for Re = 10

X/X_{out}	Cliffe	Hutton	Rasgoti	Wada	Grid 2
0.0	3.000	3.000	3.000	3.000	3.000
0.2	-0.100	-0.092	-0.080	0.152	-0.099
0.4	-0.103	-0.101	-0.103	-0.045	-0.116
0.6	0.092	0.101	0.132	0.183	0.081
0.8	0.319	0.365	0.300	0.405	0.300
1.0	0.408	0.531	0.332	0.753	0.337

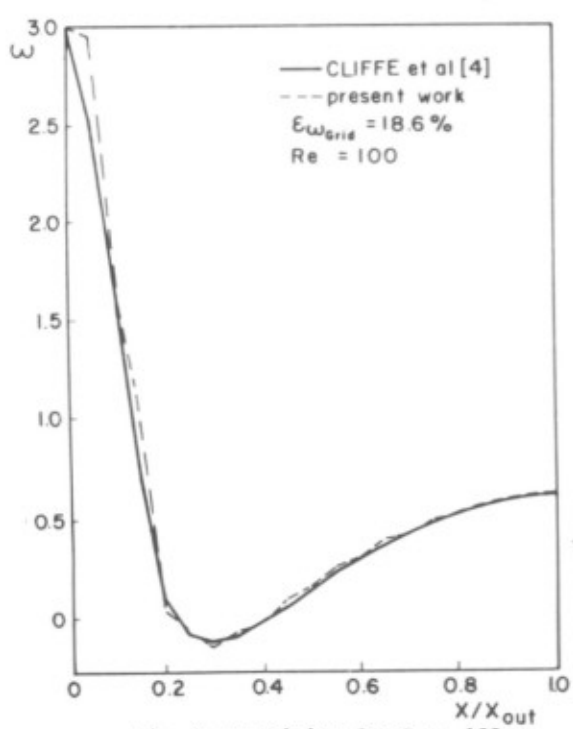

Fig. 9 Vorticity for Re = 100.

To finalize the analysis of the results, looking at Wada's results, Table I clearly demonstrates that the use of the Cartesian coordinate system is not adequate to solve fluid flow problems in complex geometries, due to the need of interpolation at the boundaries. Also in Table I are the results of Rasgoti, which uses a similar model as used in this work, but does not show a good performance as this method.

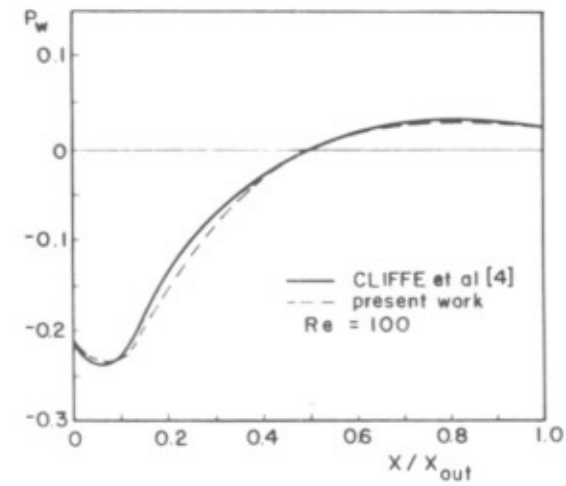

Fig. 10 Pressure for Re = 100

CONCLUSIONS

A finite volume method using general coordinate system was tested solving a laminar incompressible flow in a channel with irregular boundaries. Based on the results it was clearly demonstrated that the model described in this paper is a powerfull and general tool for predicting fluid flow problems, fitting among the best ones described in |3|, in the solution of the proposed problem.

REFERENCE

|1| De Vahl Davis, G. and Jones, I. P., Natural Convection in a Square Cavity: A Comparison Exercise, Int. J. Num. Meth. in Fluids, vol.3, pp. 227-248, 1983.

|2| Roache,P. Scaling of High Reynolds Weakly Separated Channel Flows, Symposium on Numerical and Physical Aspects of Aerodynamics Flows, 1981.

|3| Napolitano,M. and Orlandi,P. Laminar Flow in a Complex Geometry: A Comparision, Int. J. Num. Meth. in Fluids, vol. 5, pp. 667-683, 1985.

|4| Cliffe, K.A., Jackson,C.P. and Greenfield, A.C., Finite Element Solutions for Flow in a Symmetric Channel with a Smooth Expansion, AERE-R. 10608..

|5| Maliska, C.R. and Raithby, G.D., A Method for Computing Three Dimensional Flows Using Nonorthogonal Boundary-Fitted Co-ordinates, Int. J. Num. Meth. in Fluids, vol. 4, pp.519-537, 1985.

|6| Maliska, C.R. and Raithby, G.D., Calculating Three-Dimensional Flows using Nonorthogonal Grids, Numerical Methods in Laminar and Turbulent Flow, C. Taylor, J.A, Johnson and W.R. Smith, pp. 656-666, Pineridge Press, 1983.

|7| Thompson, J.F., Thames, F.C. and Mastin, C.W., Automatic Numerical Generation of Body-Fitted Curvilinear Coordinate System for Fields Containing Any Number of Arbitrary Two-Dimensional Bodies, J. Comp. Phys., vol. 15 pp.299-319, 1974.

|8| Perez, J.O., Simulação Numérica de Descargas Térmicas em Corpos d'Água Rasos de Geometria e Profundidade Variáveis, Diss. de Mestrado, Depto. Eng. Mec. Univ. Fed. Santa Catarina, junho 1987.